Third-order nonlinear spectra in C_{60} and C_{70}: Reconciling electroabsorption, third-harmonic-generation and degenerate-four-wave-mixing spectra

Bret C. Hess
Department of Physics and Astronomy,
Brigham Young University,
Provo, UT 84602

Don V. Bowersox, Shant H. Mardirosian,
and Lawrence D. Unterberger
Physics Department
California State University
Fresno, CA 93740

ABSTRACT

We present an overview of what has been learned from nonlinear optical spectral studies in C_{60} and C_{70} by our group and others. These include third harmonic generation (THG), degenerate four-wave mixing (DFWM), and electroabsorption (EA). We present empirical models of interacting states consistent with spectra of EA, THG and DFWM in C_{60} and C_{70}. The spectra in the dispersed and solid forms differ significantly. In C_{60} the lowest-energy resonances in $\chi^{(3)}(-\omega; \omega_1, \omega_2, \omega_3)$ are dominated by "forbidden" transitions made allowed by vibronic coupling in the molecule and intermolecular coupling in the solid. These interactions must be included in theoretical models of C_{60} if comparison is to be made between calculated and experimental nonlinear optical spectra. Major features of $\chi^{(3)}$ spectra in C_{70} can be modeled with similar states redshifted from those of C_{60}.

Keywords: C_{60}, C_{70}, nonlinear optics, electroabsorption, third-harmonic generation, degenerate-four-wave mixing

1. INTRODUCTION

Although the structure and composition of C_{60} and C_{70} are well known, the details of their electronic structure remain difficult to calculate with precision, because of strong electron-electron correlation effects and the large number of atoms involved. Nonlinear optical spectroscopies provide a valuable study of the electronic structure of C_{60} and C_{70}. The attempt to reproduce the nonlinear spectra theoretically is a much better test of our knowledge of their electronic structure than simply to reproduce the linear optical and electron spectroscopies, because in the nonlinear spectra dipole coupling between excited states is probed. It is well accepted that the relatively large

Downloaded From: http://proceedings.spiedigitallibrary.org/ on 04/30/2014 Terms of Use: http://spiedl.org/terms

optical nonlinearity is due to electron delocalization, as in one-dimensional conjugated polymers, and that the quasi-three-dimensional character of the molecules lowers the nonlinear response compared to the polymers. However there has been little agreement between theoretical and experimental nonlinear spectra.

Large third-order nonlinear susceptibilities $\chi^{(3)}$ have been measured[1] in films and solutions at scattered photon energies. Recent third-harmonic generation (THG) spectra of C_{60} films have been reported: Meth et al.[2] observed a THG peak at fundamental photon energy of 0.95 eV, and proposed a two-state model with a three-photon resonance to the excited state evident in the absorption peak at 2.8 eV. Kajzar et al.[3] reported peaks at both 1.2 and 0.95 eV, and proposed a three-level model with a three-photon resonance at $3\omega = 3.6$ eV (first allowed molecular transition), and a two-photon resonance at $2\omega = 1.9$ eV (lowest singlet state[4]). THG spectra in C_{70} were likewise modeled with a three-level system, with excited states near 2.5 eV.[5] A degenerate four-wave mixing (DFWM) study[6] in solid C_{60} between 1.4 and 1.7 eV has found the signal decreases toward higher energies, signifying a resonance below 1.4 eV. DFWM studies in C70 films[1] show magnitudes similar to those of C60, but with an almost flat response over the same spectral range. DFWM data in solid C_{60} and C_{70} from several references have recently been renormalized to a common standard, and compared to THG magnitudes.[1] This comparison shows an overall similarity between the nonlinear response of C_{60} and C_{70} in the range studied.

We recently reported electroabsorption studies in C_{60} and C_{70}.[7] Unlike the above studies, we took spectra in both dispersed and solid fullerenes, and observed large differences in the spectra of the two forms.

Electroabsorption (EA) probes the same interactions between excited states as does THG and DFWM, but displays only one-photon resonances. EA is given by $\mathrm{Im}[\chi^{(3)}(-\omega;\omega, 0,0)]$, THG by $|\chi^{(3)}(-3\omega;\omega,\omega,\omega)|$, and DFWM by $|\chi^{(3)}(-\omega;\omega, \omega,-\omega)|$. EA has the advantage of a broad, continuous energy range and good signal to noise. It also gives phase information difficult to obtain from pulsed laser spectroscopies because $\mathrm{Im}[\chi^{(3)}]$ includes both positive and negatives signals as opposed to the THG and DFWM spectra which usually probe only the magnitude of $\chi^{(3)}$. EA in solid C_{60} was measured[8,9] soon after thin films of C_{60} were available. EA in solid C_{70} was shown over a narrow spectral range[10]. Other EA studies of solid C_{60} and C_{70} remain unpublished.[10] EA of C_{60} in polysilane was reported[11], but the polysilane EA masked most of the C_{60} EA. Our focus has been to try to understand in a consistent way all three available spectra: EA, DFWM and THG. In this paper we review the analysis presented for C_{60}, and extend a similar empirical model to C_{70}, and discuss the similarities and differences in the two.

2. EXPERIMENT

C_{60} (C_{70}) films from 99.9% (98%) powder were evaporated from a quartz crucible near 450 °C. Dispersed samples were prepared from toluene solutions of the fullerene mixed with poly(methyl-methacrylate)[12] dissolved in warm toluene (fullerene: PMMA≈1:100 by weight). This was cast on

Downloaded From: http://proceedings.spiedigitallibrary.org/ on 04/30/2014 Terms of Use: http://spiedl.org/terms

substrates and the toluene was removed under vacuum. The spectra of dispersed samples of C_{60} (C_{70}) in PMMA in our spectral range is essentially identical[12] to that of C_{60} (C_{70}) in toluene solution, and have no solid-state features. Al electrodes were used to apply fields of 10^4 - 10^5 V/cm at 1.5 kHz. The light source was a Xe lamp and a 1/4 m monochromator. Changes (ΔT) in transmission with field were normalized by the transmitted light (T) to form the EA spectrum $-\Delta T/T$, which is proportional to the change in absorption, neglecting any change in reflectance. A Si detector was used with a lockin amplifier. Near 4.2 eV, PMMA has some EA, which was subtracted.

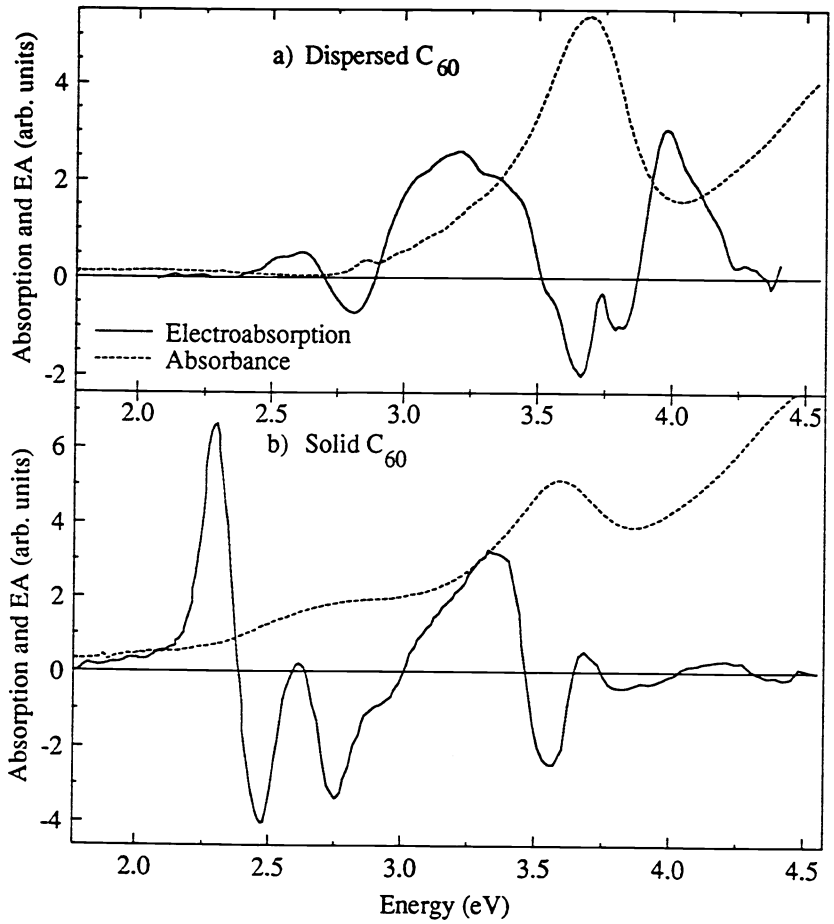


FIG. 1. Measured electroabsorption and linear optical absorption in C_{60}: a) C_{60} dispersed in PMMA; b) solid C_{60} film. Note that there is no EA resonance at the lowest singlet transition near 1.9 eV.

Fig. 1 shows the optical absorption and EA spectra of C_{60}, for dispersed molecules and films. The expected EA features are 1) a transfer of oscillator strength, giving positive ($\Delta\alpha > 0$) and negative EA peaks at transitions exchanging strength; 2) Stark-shifting of allowed transitions, giving structures similar to the first derivative of the shifted absorption feature; and 3) second-derivative-like structures, which will be discussed below. Although the features can be interpreted in different ways, we present here our interpretation of the EA spectra and their changes between

Downloaded From: http://proceedings.spiedigitallibrary.org/ on 04/30/2014 Terms of Use: http://spiedl.org/terms

samples as motivation for our model. Both the C_{60} film and molecule show EA derivative structures near the T_{1u} absorption peaks at 3.6 and 3.7 eV, respectively (we use total electron symmetry notation: A_g is the ground state; only A_g-T_{1u} transitions are dipole allowed without vibronic or solid state perturbations). This main T_{1u} feature in the range 3-4 eV is closer to the second derivative[10,13] of the absorption than it is to the first derivative, evidenced by the negative EA peak at the position of the absorption peak, and positive peaks on either side. The EA features associated with symmetry-forbidden states are also of interest. In both the film and the molecule, there is a negative EA peak near 2.8 eV. An enhancing peak at 2.6 eV appears in the molecule, but in the film this feature becomes a strong red-shifting derivative structure at 2.4 eV; the change to derivative EA occurs as the transition becomes allowed in the solid, and then is Stark-shifted by the applied field. Note that no EA is seen near the energy of the lowest singlet excited state at 1.9 eV,[4] indicating that this state plays little role in the nonlinear optical properties of C_{60}.

The second-derivative-like (broadening) nature of the T1u EA in C_{60} near 3.6 eV has several possible origins: EA of 1) disordered permanent dipoles, 2) charge-transfer states[13], and 3) an allowed state coupled strongly to a second close-lying state. The only permanent dipoles possible in C_{60} would be from extrinsic defects, but because of the similarities of the EA at 3.6 eV between the very different film and dispersed samples, an extrinsic mechanism is unlikely. We can reject charge-transfer states as the explanation for the feature near 3.6 eV because the feature is seen in the dispersed sample, whereas charge-transfer states should occur only in solid C_{60} between molecules. Hence we suggest that the broadening is caused by a nearby state that is dipole-coupled to the T_{1u} state. This is confirmed by recent calculations of EA in C_{60}, where a second derivative feature was observed at the dominant low-energy T_{1u} peak .[14]

The EA and absorption spectra for dispersed and solid C_{70} is shown in Fig. 2. The most obvious differences between the spectra in C_{60} and C_{70} are a general redshifting of spectral features, and the increasing complexity in the spectra due to the lower symmetry in C_{70}. However, there are important similarities between the two. 1) There is a strong feature at about 3.2 eV in the dispersed C_{70} EA, which may be analogous to the T_{1u} EA feature in C_{60} near 3.6 eV (in solid C_{70} this strong feature is not present; instead only small oscillatory features are seen). 2) At the lowest energies, the EA is generally enhancing: the positive feature at 2.6 eV in the dispersed C_{60} EA appears to have its analog in (or among) the several positive peaks between 1.8 and 2.2 eV in dispersed C_{70}. 3) The positive feature near 2.2 eV in dispersed C_{70} becomes a strong derivative-like structure in solid C_{70}, just as in C_{60} the lowest enhancing EA feature (2.6 eV) becomes a strong derivative structure in the transition to the solid (2.4 eV). 4) Between these high and low energy features is a negative feature in the molecule; in C_{70} this appears at about 2.6 eV, redshifted from the similar feature in C_{60} at 2.8 eV. In solid C_{70}, this apparently becomes the smaller derivative structure near 2.45 eV.

We note that the strong T_{1u}-like derivative feature seen at 3.2 eV in dispersed C_{70} appears to have disappeared in sold C_{70}, replaced by gentle oscillations. This was also observed in other work[10].

Downloaded From: http://proceedings.spiedigitallibrary.org/ on 04/30/2014 Terms of Use: http://spiedl.org/terms

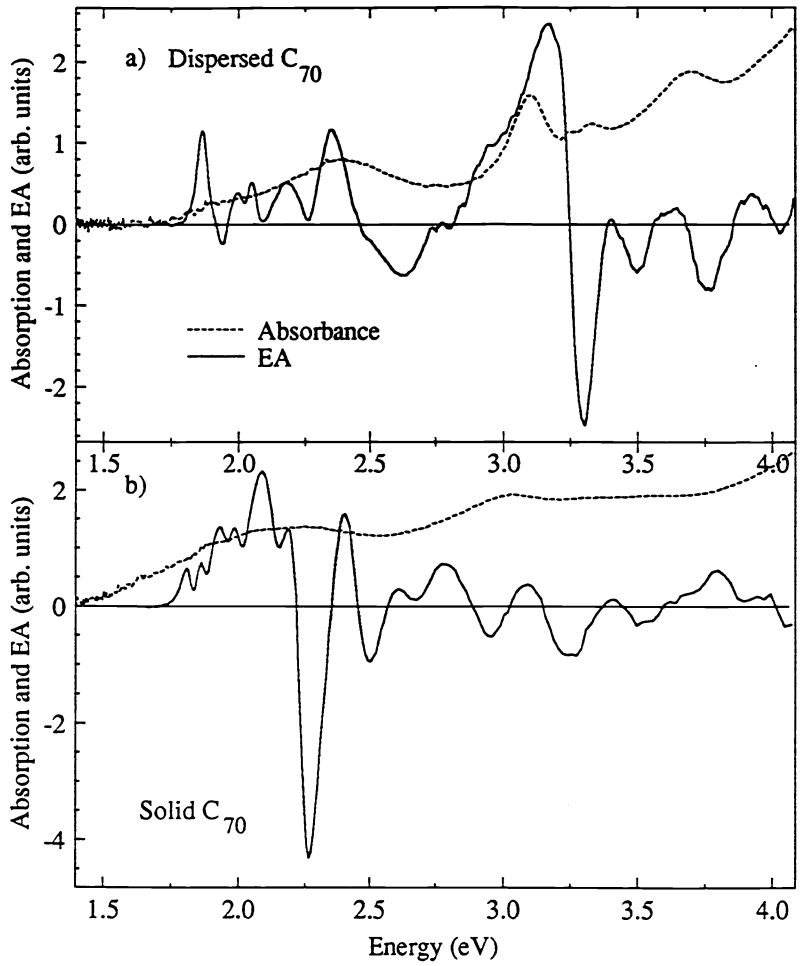


FIG. 2. Electroabsorption and linear optical absorption in C_{70}: a) C_{70} dispersed in PMMA; b) solid C_{70} film.

3. DISCUSSION

As we discussed earlier[7], available theoretical calculations do a poor job of modeling the experimental nonlinear spectra in the fullerenes, due to poor modeling of the lowest energy states and the neglect of vibronic and solid-state coupling in the spectra.

In the absence of theoretical spectra that could be compared with experiment, we proposed[7] an empirical model of several interacting states consistent with EA, THG and DFWM in C_{60}. Here we also present a model for C_{70}. We used the standard perturbation theory results[15,16] for $\chi^{(3)}$

Downloaded From: http://proceedings.spiedigitallibrary.org/ on 04/30/2014 Terms of Use: http://spiedl.org/terms

$$\chi^{(3)}(-\omega;\omega_1,\omega_2,\omega_3) \propto -\mathbf{P}_{1,2,3}\{\sum_{\substack{m,n,p \\ n\neq g}} \mu_{gm}\mu_{mn}\mu_{np}\mu_{pg} \times$$

$$[\frac{1}{(E_m-\omega)(E_n-\omega_1-\omega_2)(E_p-\omega_1)}+\frac{1}{(E_m{}^*+\omega_3)(E_n-\omega_1-\omega_2)(E_p-\omega_1)}+$$

$$\frac{1}{(E_m{}^*+\omega_1)(E_n{}^*+\omega_1+\omega_2)(E_p-\omega_3)}+\frac{1}{(E_m{}^*+\omega_1)(E_n{}^*+\omega_1+\omega_2)(E_p{}^*+\omega)}]$$

$$-\sum_{m,n}\mu_{gm}^2\mu_{gn}^2[\frac{1}{(E_m-\omega)(E_m-\omega_3)(E_n-\omega_1)}+\frac{1}{(E_m-\omega_3)(E_n{}^*+\omega_2)(E_n-\omega_1)}+ \quad (1)$$

$$\frac{1}{(E_m{}^*+\omega_3)(E_n-\omega_2)(E_n{}^*+\omega_1)}+\frac{1}{(E_m{}^*+\omega)(E_m{}^*+\omega_3)(E_n{}^*+\omega_1)}]\}$$

which sums over singlet excited states m, n, and p; g denotes the ground state A_g. μ_{mn} is the dipole coupling between states m and n. Damping Γ is included by replacing E_m by $E_m + i\Gamma$. $\mathbf{P}_{1,2,3}$ is the average of permutations over indices 1,2,3. EA is given by $\mathrm{Im}[\chi^{(3)}(-\omega;\omega, 0,0)]$, THG by $|\chi^{(3)}(-3\omega;\omega,\omega,\omega)|$, and DFWM by $|\chi^{(3)}(-\omega;\omega, \omega,-\omega)|$. We focused only on the spectral shape, using relative transition strengths μ_{mn}.

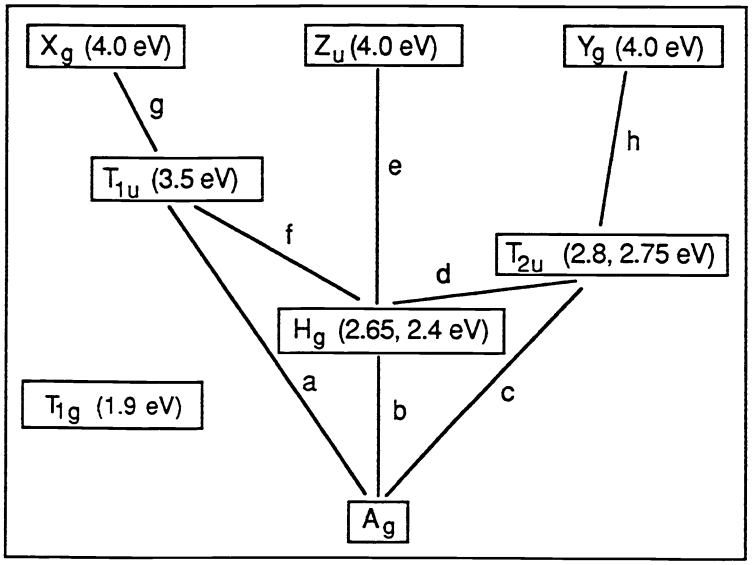


FIG. 3. Model of interacting singlet states for $\chi^{(3)}$ in C_{60}. Lines are dipole coupling for a model consistent with EA, THG and DFWM. The lowest singlet excited state at 1.9 eV [4] is shown, but is not coupled to the states in the model because the lack of EA at 1.9 eV in dispersed C_{60} shows that its contribution to $\chi^{(3)}$ is small.

Downloaded From: http://proceedings.spiedigitallibrary.org/ on 04/30/2014 Terms of Use: http://spiedl.org/terms

The lines between states in Fig. 3 depict dipole couplings in our model for EA, THG and DFWM spectra in C_{60}. For the states H_g and T_{2u}, the two energies listed are for the molecule and the solid respectively; the small solid-state energy shifts of the other states are neglected. Model energy levels for the dispersed form (2.65, 2.8, 3.5 eV) are almost identical to theoretical[17] H_g, T_{2u}, and T_{1u} levels: 2.65, 2.8, and 3.4 eV, respectively; hence our labeling. The states X_g , Y_g and Z_u are unidentified higher-energy states (or may each represent several states) that dipole couple to T_{1u}, T_{2u} and H_g respectively. These higher-energy states are essential to model the EA near the T_{1u} and T_{2u} transitions. They are placed in our model at 4.0 eV because of the EA features seen near 4.0 eV and the strong two-photon enhancement in the DFWM near 2.0 eV. The X_g and Y_g are represented as separate states because under icosohedral symmetry, the T_{2u} and T_{1u} states dipole couple to different sets of even parity excited states.

The relative dipole elements μ_{mn} in Fig. 3 are given by the parameters a-h, and are shown in Table 1 (note that the value of h was listed incorrectly in [7]). The dipole moments that couple with the ground state (a,b,c) were chosen to be consistent with the strength of linear absorption features in the dispersed form and solid. For the solid, only the coupling of the ground state to the two lowest (forbidden) states change in our model: b(0.3) and c(0.53), consistent with the increase in absorption to these states in the solid. The remaining five dipole moments (d-h), which couple excited states, were chosen to give reasonable agreement with the EA, THG and DFWM. For all states the broadening was $\Gamma = 0.1$ eV.

	a	b	c	d	e	f	g	h	T_{1u}	H_g	T_{2u}
C_{60} dispersed	1	0	.13	.7	2.7	.1	.75	1.4	3.5 eV	2.65 eV	2.8 eV
film		.3	.53							2.4 eV	2.75 eV
C_{70} dispersed	1	0	.53	.5	2	0	1.5	2.3	3.2 eV	2.2 eV	2.45 eV
film		.7									

Table 1. Parameters used in the model of $\chi(3)$. a-h are relative dipole matrix elements; the energies of excited states are listed under the state label. For the film an empty space indicates that the parameter value is the same as that used for the dispersed form.

Given the qualitative similarities between the nonlinear spectra in C_{60} and C_{70}, we modeled the nonlinear spectra in C_{70} with a set of states similar to those used for C_{60}, allowing for redshifts and changes in oscillator strength. Thus we use the same diagram (Fig 3) to discuss the model for C_{70}. In C_{70}, we place a T_{1u}-like state at 3.2 eV, a T_{2u}-like state at 2.45 eV, an H_g-like state near 2.2 eV. This represents of redshift of close to 0.4 eV of these states in going from C_{60} to C_{70}. The states X_g, Y_g, and Z_u are left in place at 4 eV. The parameters of the model for C_{70} are

Downloaded From: http://proceedings.spiedigitallibrary.org/ on 04/30/2014 Terms of Use: http://spiedl.org/terms

summarized in Table 1. The relative oscillator strengths for C_{70} have weightings not unlike those for C_{60}, given above. For solid C_{70}, the only change in the model is the onset or increase of absorption to the H_g-like 2.2 eV state, reflected by increasing the parameter b to 0.7. Even though the large EA feature near 3.2 eV is lost in the transition from dispersed to solid C_{70}, we believe that the coupling between excited states on one molecule are not perturbed strongly as intermolecular coupling appears in the solid. The broadening was again 0.1 eV.

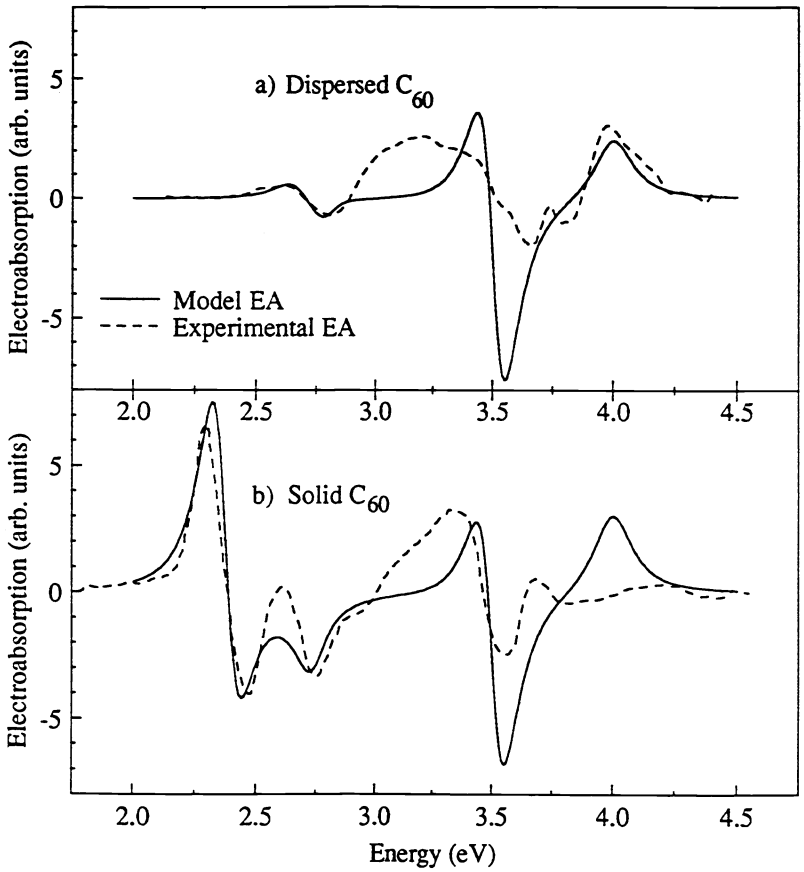


FIG. 4. Calculated (solid line) and experimental (dashed line) EA spectra a) of solid C_{60} and b) of dispersed C_{60}.

Figures 4 and 5 show the model and experimental EA spectra for both C_{60} and C_{70}. Within our model for dispersed C_{70} (Fig. 5), the H_g-like state at 2.2 eV receives oscillator strength from its coupling to the T_{2u} - and the Z_u- like states. In the solid, the absorption transition at 2.2 eV is stronger, and this coupling now causes a redshifting derivative to appear at 2.2 eV. At 2.5 eV, in both the molecule and solid, the T_{2u}-like state shows a redshifting derivative structure due to its coupling to the higher Y_g state(s). The T_{1u}-like state is repelled by its interaction with the higher state at 4 eV. These are qualitatively similar to the results obtained for C_{60}, except that in C_{60} the T_{2u} state simply loses oscillator strength instead of being redshifted, because of its nearly balancing interactions between the H_g and Y_g states.

Downloaded From: http://proceedings.spiedigitallibrary.org/ on 04/30/2014 Terms of Use: http://spiedl.org/terms

This simple model does less well above 3 eV in solid C_{70}, because it cannot explain the loss of the strong feature seen in dispersed C_{70}.

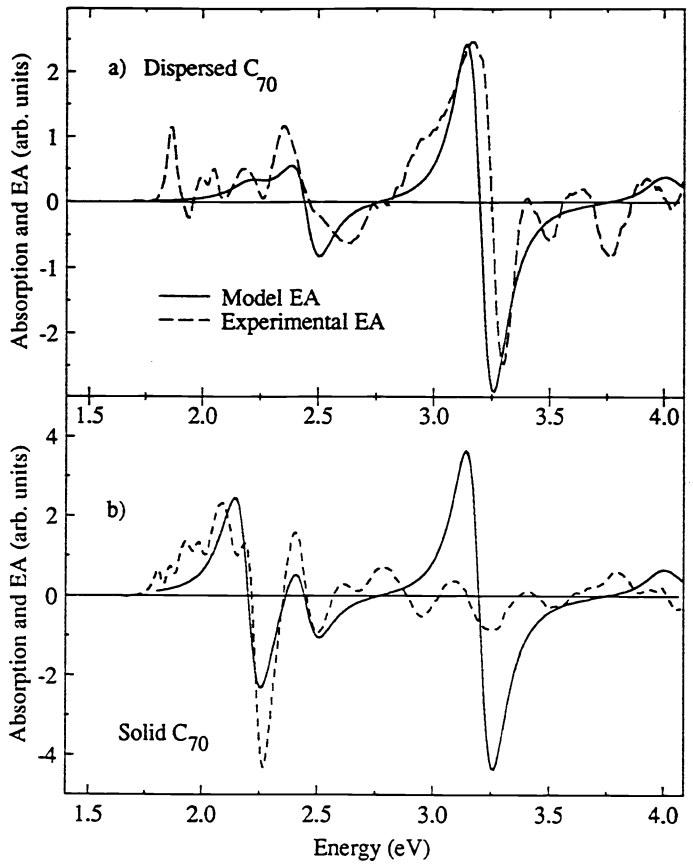


FIG. 5. Calculated (solid line) and experimental (dashed line) EA spectra a) of solid C_{70} and b) of dispersed C_{70}.

The THG spectra agree quite well with experiment (Fig 6). The 1.2 eV peak comes from a two-photon resonance to 2.4 eV and from a three-photon resonance to the 3.6 eV level; thus there is a double resonance here. This large peak is mostly due to channels a-f-d-c, and c-d-d-c, (see Fig 3), which are much larger in the solid than in the molecule because of the increase in c. The strong transitions a-g-g-a and a-a-a-a essentially cancel. At lower energies, there are three-photon resonances at 0.8 and 0.93 eV to the 2.4 and 2.8 eV states respectively. In solid C_{70}, similar features are seen. The peaks near 0.7 and 0.8 eV are again three-photon resonances to the lowest two states in the model. Near 1.1 eV, we again have a double resonance: two-photon resonance to 2.2 eV, and a three-photon resonance to 3.2 eV. In the C_{70} molecule the three-photon resonance dominates, because a-g-g-a is almost three times as large as a-a-a-a. In the C_{70} solid, absorption to the H_g-like state at 2.2 eV increases, and causes new transitions which tend to cancel the three-photon resonance.

Downloaded From: http://proceedings.spiedigitallibrary.org/ on 04/30/2014 Terms of Use: http://spiedl.org/terms

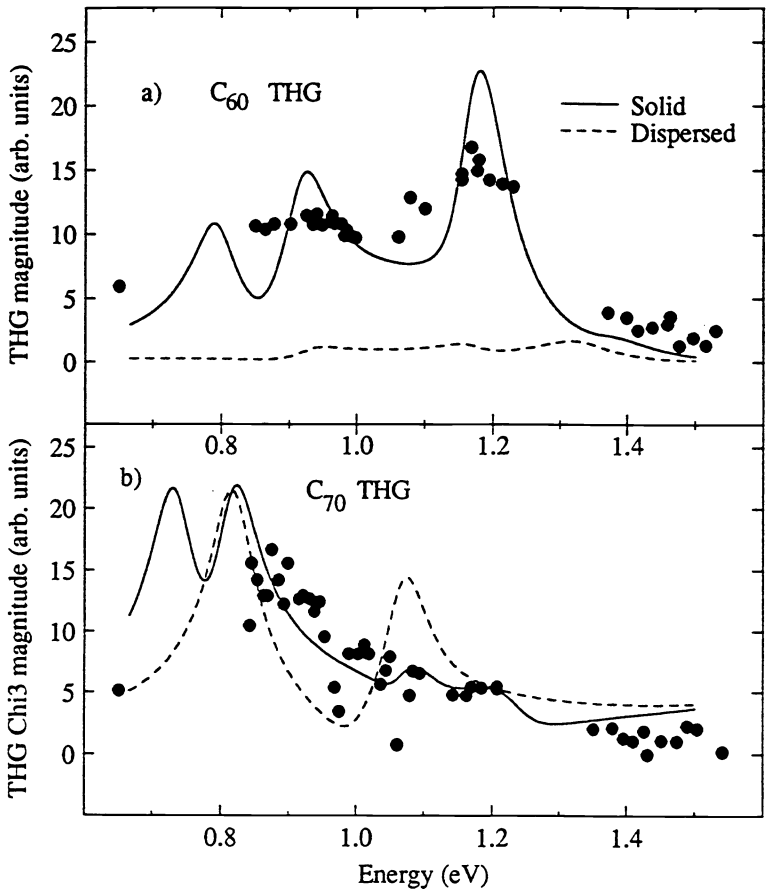


FIG. 6. a) Calculated THG spectra of solid C_{60} (solid line) and of dispersed C_{60} (dashed line), and of b) solid and dispersed C_{70}. The points are experimental data from Kajzar et al [3,5], all for solid films.

Fig 7 shows the calculated and available DFWM spectra in C_{60} and C_{70}. For C_{60}, our model shows that two-photon resonances at 1.2 and 1.4 eV (to the H_g and T_{1u} states) are responsible for the decrease in the DFWM signal measured by Strokendl et al[1] from 1.4 to 1.7 eV. Note that we use the renormalized data of [1]. Two-photon resonances to the X_g, and Y_g, near 4.0 eV give the large enhancement of the DFWM near 2 eV as measured by Flom et al.[18] Note that near 1.6 eV the slope of the calculated DFWM spectra for the solid is opposite that observed in experiment. This is due to the unrealistically broad tails calculated for the one-photon resonance at 2.4 eV. Our simple model allows only homogeneous broadening and gives Lorentzian-like lines with broad tails (when a Lorentzian line is artificially broadened to a width $\Gamma=\Delta\omega$ to represent inhomogeneous broadening of width $\Delta\omega$, the nonresonant $\chi^{(3)}(0)$ of this line is incorrectly multiplied by about $\Delta\omega/\delta\omega$, where $\delta\omega$ is the true homogeneous linewidth within the inhomogeneous envelope; for C_{60}, $\delta\omega$ is probably much less than the $\Gamma=0.1$ eV used here).

Downloaded From: http://proceedings.spiedigitallibrary.org/ on 04/30/2014 Terms of Use: http://spiedl.org/terms

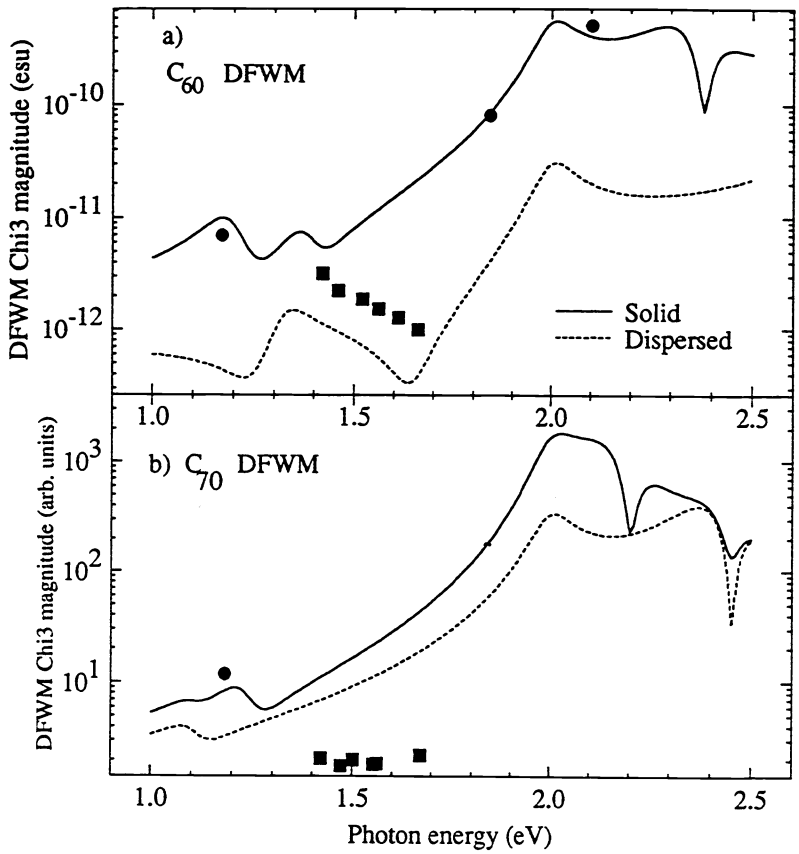


FIG. 7. Calculated DFWM spectra a) of solid C_{60} (solid line) and of dispersed C_{60} (dashed line), and b) of solid and dispersed C_{70}. The square points are experimental data for $\chi^{(3)}_{xxxx}$ from [1,6]; the circles are $\chi^{(3)}_{xxxx}$ from [18], all for solid films. The calculated curves (arbitrary units) are multiplied by a common factor for comparison with the data.

The most recent DFWM data on solid C_{60} by Strokendl et al[19] (not shown in Fig. 7) is fully consistent with our model, and agree with the solid curve in Fig 7a, within the experimental resolution. In a study of DFWM below 1.4 eV, they find a broad peak in solid C_{60} in the same region as the peaks we calculate near 1.2 eV, and no peak at 0.95 eV. Because three-photon resonances do not occur in DFWM, this shows that (in contrast with the model presented by Kajzar et al[3]) there are two-photon resonances near 1.2 eV to the excited state at 2.4 eV. In addition, any two-photon transitions to the 1.9 eV state have a small influence on the spectrum since a resonance is not seen at 0.95 eV, all of which is consistent with our model and what we observe in EA.

In C_{70}, there is little DFWM data (Fig 7b). But we can understand the negligible slope in the DFWM data near 1.5 eV, compared to the significant slope seen in solid C_{60}. In C_{70} the lower energy resonances are farther away from 1.5 eV, and the higher-energy resonances are closer, both of which would cause the slope to become less negative with energy. Again, the model predicts

Downloaded From: http://proceedings.spiedigitallibrary.org/ on 04/30/2014 Terms of Use: http://spiedl.org/terms

resonances near 1.1-1.2 eV, which is consistent with the few points available. The previous comments regarding the unrealistically broad tails in model apply here as well.

Although our simple model gives insights into the resonances observed in THG, DFWM and EA, it is clearly not a substitute for a true theoretical description. To better model the experimental spectra, we suggest an emhasis on a better description of the lowest electronic states and including vibronic structure in calculations of $\chi^{(3)}(-\omega; \omega_1, \omega_2, \omega_3)$. Since we have shown that the lowest nonlinear optical resonances in EA, DFWM, and THG in dispersed C_{60} involve transitions that are allowed only by vibronic coupling to dipole forbidden states, vibronic interactions must be included in a reasonable calculation of the spectra. To better describe the lowest electronic states, our first suggestion[7] was that *ab initio* calculations would be necessary, because in the semiempirical calculations[17], the lowest singlet states are crowded around 2.3 eV. We are more concerned with the spacing between these lowest states than we are in their absolute energies. In dispersed C_{60}, the experimental results[4,7] show that the spacing between the states T_{1g} - H_g-T_{2u}-T_{1u} is about 0.7, 0.2, 0.8 eV respectively. We have since come across an *ab initio* calculation of C_{60}[20], and indeed the spacing of these states (0.7, 0.3, 1.3 eV) is much improved over the semiempirical calculations[17], so perhaps $\chi^{(3)}(-\omega; \omega_1, \omega_2, \omega_3)$ from *ab initio* calculations will offer a much better understanding of the details of the nonlinear optical response of C_{60} and C_{70}. When these issues are adequately addressed in dispersed C_{60} and C_{70}, we will have hope that calculations of solid state spectra will be meaningful. The experiments reviewed here should serve as a useful guide to evaluate the success of such calculations in describing electron-electron correlation in these fascinating molecules.

In conclusion, we report the first third-order nonlinear optical spectra in both dispersed and solid states of fullerenes in the form of electroabsorption, and find large vibronic and solid state effects. We give a simple empirical model consistent with EA, DFWM and THG spectral data. The excited states near 2.4, 2.8, and 3.6-4.0 eV play a large role in the nonlinear spectra of C_{60}.

4. ACKNOWLEDGMENTS

We are grateful for many helpful discussions with S. Abe, K. Harigaya, S. Jeglinski and Z. V. Vardeny. This research was supported in part by a grant from Research Corporation.

Downloaded From: http://proceedings.spiedigitallibrary.org/ on 04/30/2014 Terms of Use: http://spiedl.org/terms

5. REFERENCES

1. For a review, see F. P. Strokendl, R. J. Larsen, Theresa J. Axenson, L. R. Dalton, H. W. Sarkas, and Z. H. Kafafi, Fullerenes and Photonics II, SPIE Vol 2530, 1995, p. 165, and references in [3].
2. J. S. Meth, H. Vanherzeele and Y. Wang, Chem. Phys. Lett. 197 (1992) 26.
3. F. Kajzar, C. Taliani, R. Danieli, S. Rossini, and R. Zamboni, Chem. Phys. Lett. 217 (1994) 418.
4. Z. Gasyna, P .N. Schatz, J. P. Hare, T. J. Dennis, H. W. Kroto, R. Taylor, and D. R. M. Walton, Chem. Phys. Lett. 183 (1991) 283.
5. F. Kajzar, C. Taliani, R. Danieli, S. Rossini, Phys. Rev. Lett 73 (1994) 16174
6. F. P. Strohkendl, R. J. Larsen, L. R. Dalton, R. W. Hellwarth, H. W. Sarkas, and Z. H. Kafafi, SPIE vol. 2284 Fullerenes and Photonics (1994) 78.
7. B. C. Hess, D. V. Bowersox, S. H. Mardirosian, and L. D. Unterberger, Chem. Phys. Lett.248 (1996) 141.
8. K. Pichler, S. Graham, O. M. Gelsen, R. H. Friend, W. J. Ramavow, J. P. McCauley Jr, N. Coustel, J.E. Fischer, and A. B. Smith III, J. Phys.: Condens. Matter 3 (1991) 9259 .
9. S. Jeglinski, Z. V. Vardeny, D. Moses, V. I. Sradanov, and F. Wudl, Synth. Met. 49-50 (1992) 557.
10. S. Jeglinski, Ph.D. Thesis, University of Utah, Physics Department, 1996,unpublished; X. Wei, S. Jeglinski, O. Paredes, Z. V. Vardeny; D. Moses, V. I. Srdanov, G.D. Stucky, K. C. Khemani, and F. Wudl, Solid State Communications, vol.85, no.5, p. 455-9.
11. R. G. Kepler and P. A. Cahill, Appl. Phys. Lett., 63 (1993) 1552.
12. M. Gevaert and P.V. Kamat, J. Phys. Chem. 96 (1992) 9883.
13. P. Petelenz, M. Slawik, and B. Pac, Synthetic Metals, 64, (1994) 335.
14. S. Abe et al, these proceedings.
15. B. J. Orr, and J. F. Ward, Mol. Phys. 20 (1977) 513.
16. S. Abe, Relaxation in Polymers, ed. by T. Kobayashi (World Scientific).
17. F. Negri, G. Orlandi, and F. Zerbetto, J. Chem. Phys. 97 (1992) 6496.
18. S. R. Flom, R.G.S. Pong, F. J. Bartoli and Z. H. Kafafi, Mol. Cryst. Liq. Cryst. 256 (1994) 289; .J. R. Lindle, R.G.S. Pong, F. J. Bartoli and Z. H. Kafafi, Phys. Rev. B 48 (1993) 9447.
19. F. P. Strohkendl et al, these proceedings.
20. H. Weiss, R. Ahlrichs, and M. Haser, J. Chem. Phys. 99 (1993) 1262

Downloaded From: http://proceedings.spiedigitallibrary.org/ on 04/30/2014 Terms of Use: http://spiedl.org/terms